Proceedings of CONF-MCEE 2027 Symposium: Innovative Environmental Engineering Strategies for a Sustainable Future
DOI: 10.54254/2755-2721/2027.MA38676

Urban Greenness and Summer Land Surface Temperature: Evidence from a 1-km Grid Panel of Berlin, Budapest, and Vienna

Zhiwei Li

Faculty of Engineering, University of Nottingham, Nottingham, UK
alyzl97@nottingham.ac.uk

Abstract. Urban greening is commonly promoted as a heat-mitigation strategy, but most of the remote-sensing evidence is cross-sectional and thus makes the vegetation image associated with persistent differences in urban form and location. In this study, we build a 2012-2021 summer panel of 1,818 one-kilometre grids across Berlin, Budapest, and Vienna, with 18,156 grid-year observations. Using grid fixed effects, city-by-year fixed effects, ERA5 weather controls, and grid-clustered standard errors, we estimate the annual summer LST to be related to the Normalized Difference Vegetation Index (NDVI) with a 0.1 increase in NDVI (SE = 0.033) and a 0.835 °C reduction in the summer LST (SE = 0.033). The estimation is stable when boundary-area weights are used, interior grids are limited, balanced panels are used, winsorization is used, and Driscoll-Kraay inference is performed. The city-specific estimates are -0.708 °C in Berlin, -0.930 °C in Budapest, and -0.739 °C in Vienna. The MODIS data show that a higher NDVI is associated with richer evapotranspiration and latent heat flux, as expected from an evaporative cooling channel, but the missing values over an otherwise impervious surface will not be used in the formal mediation case. The cooling is weaker in grids with high 2020 built-up fractions. In contrast, the lagged NDVI is not significant, and the estimates should be considered to be robust within-grid contemporaneous associations rather than causal effects. The results indicate that greening can be achieved from a spatial perspective and support the use of policy-based quasi-experimental designs and better time-varying measures of the green space structure.

Keywords: urban green space, land surface temperature, NDVI, fixed effects, evapotranspiration

1. Introduction

Cities modify the surface energy balance through impervious materials, reduced evapotranspiration, aerodynamic roughness, and storage and release of sensible heat. These processes produce urban thermal environments that can amplify heat exposure, energy demand, and health risks [1-5]. As vegetation absorbs solar radiation, provides shade, and converts available energy into latent heat through evapotranspiration, urban greening is one of the key drivers of climate adaptation. However,

© 2026 The Authors. This is an open access article distributed under the terms of the Creative Commons Attribution License 4.0 (https://creativecommons.org/licenses/by/4.0/).

DOI: 10.54254/2755-2721/2027.MA38676

this approach varies from one climate to another and even by the vegetation types it may be effective.

Satellite-based LST and vegetation indices have enabled us to monitor thermal conditions in large areas. A large body of literature has shown negative spatial relationships between LST, vegetation, and landscape composition [6, 7], lower temperatures in and around parks and other green or blue spaces [8, 9], and interactions between canopy cover and impervious surfaces [10]. European evidence also shows that urban trees are significantly cooler than continuous urban fabric and that the degree of cooling varies from region to region [11]. These studies demonstrate the physical plausibility and planning significance of green space cooling.

Nevertheless, there are three common problems. First and foremost, many studies use one or only a few satellite scenes, and it is difficult to separate vegetation from longer-term spatial features, such as elevation, location, centrality, building density, and proximity to water. Second, evidence is usually given for a single city only, and we do not know if coefficients can be generalized to other cities. Third, mechanism claims are often based on theory, not on evapotranspiration or latent-heat information. Such limitations matter because the gradients in vegetation–temperature in the area of the vegetation are not expected to match the cooling that will occur with vegetation that has changed over time in the same location.

The present paper fills these gaps by using a harmonized 10-year grid panel with three Central European capitals and a regional grid at each city. The analysis makes four contributions: grid fixed effects remove all time-invariant local characteristics, and city-by-year fixed effects absorb city-wide annual shocks. Second, daily ERA5 data control for spatially varying summer meteorology. Third, MODIS evapotranspiration and latent heat products provide additional evidence on the evaporative pathway. Fourth, the common design allows direct comparison between Berlin, Budapest and Vienna and to see if the association varies by built-up intensity.

The best estimate was that a 0.1 increase in NDVI is associated with a 0.835 °C decrease in summer LST. This result is consistent for several different specifications, but the lack of a significant lagged-NDVI effect should be interpreted with caution. The present paper therefore distinguishes between a strong cooling relationship and a policy treatment effect.

2. Literature review and hypotheses

2.1. Biophysical pathways

Vegetation affects surface temperature in several ways. Shading reduces incoming shortwave radiation on the ground and building surfaces. Evapotranspiration changes available energy from sensible to latent heat (strength of this energy depends on soil moisture, atmospheric demand and plant physiology), vegetated surfaces are also different from construction materials in albedo, emissivity, thermal inertia and roughness. These processes suggest that abundance of vegetation should be negatively associated with daytime summer LST, but they also suggest context dependence: cooling may be moisture limited and trees can behave differently from grass or cropland.

Hypothesis 1 (cooling association). In the same 1-km grid, higher summer NDVI is associated with lower summer LST after accounting for common annual shocks and meteorological conditions.

DOI: 10.54254/2755-2721/2027.MA38676

2.2. Evapotranspiration as a mechanism

The latent-heat pathway is central to explaining vegetative cooling. MODIS evapotranspiration estimates are based on vegetation condition and meteorological demand [12]. European evidence also shows spatial variation in tree cooling associated with evapotranspiration [11]. Then a mechanism consistent pattern would require both a positive NDVI–evapotranspiration association and negative evapotranspiration–LST association.

Hypothesis 2 (evaporative pathway). Higher NDVI is related to higher evapotranspiration and latent heat flux which are also related to lower LST.

2.3. Urban-form and city heterogeneity

Cooling performance may vary between cities because background climate, water availability, vegetation and urban form all affect the surface energy balance [11, 13]. At smaller scales canopy and impervious cover interact nonlinearly [10]. High built-up intensity can reduce vegetation size and soil volume, decrease moisture availability and increase heat storage; shade is also important in dense areas.

Hypothesis 3 (context dependence). The NDVI–LST association is different in cities and grids with low and high intensity.

3. Data and empirical strategy

3.1. Study area and panel construction

The study covers the administrative areas of Berlin (Germany), Budapest (Hungary) and Vienna (Austria). Each city is organized into a grid (with grid coordinates) of 1 km in the European Lambert Azimuthal Equal Area coordinate system (EPSG:3035). Geographical information of each city and corresponding grid coordinates will make it easier to link data with external data. The observation period is 2012–2021 and summer is from 1 June to 31 August every year.

The core panel contains the annual summer mean LST and NDVI for each grid and the fraction of the 1-km cell inside the administrative boundary. The analysis sample includes 888 grids in Berlin, 512 in Budapest and 418 in Vienna. Berlin and Budapest are balanced 10-year panels. Vienna contains 4,156 out of 4,180 possible grid-year data, and there are 24 missing data points. LST and NDVI have no missing records. Figure 1 shows the spatial distribution of long-run mean summer LST across the study grids.

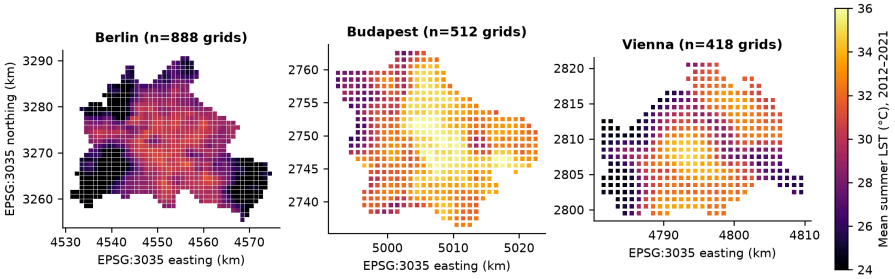


Figure 1. Spatial distribution of long-run mean summer LST

Note: Each square represents one 1-km administrative-area grid. The values are grid means for the observed summers between 2012 and 2021. Coordinates are EPSG:3035.

DOI: 10.54254/2755-2721/2027.MA38676

The LST and NDVI variables were provided as preprocessed annual summer means. The CSV files do not contain upstream satellite products, cloud and shadow masks, emissivity correction, valid-observation counts, acquisition date distribution, or compositing algorithm. This is not a problem for the panel estimations presented here, but we need to add these processing details to the final reproducibility statement.

3.2. Supplementary covariates

The daily meteorological controls are from ERA5, the ECMWF reanalysis carried out by the Copernicus Climate Change Service [14]. The grid centres were connected with the nearest 0.25° ERA5 cell. The 1,818 study grids correspond to 15 weather cells. Daily results were collected over June-August to get mean 2 m air temperature, total precipitation, mean shortwave radiation, mean 10 m wind speed, mean relative humidity, reference evapotranspiration, and extreme temperature. If we do not keep a weather cell with 1 km resolution, we do not have to keep reanalysis fields.

The mechanisms are estimated by annual actual evapotranspiration, potential evapotranspiration, latent heat flux, and temperature flux from NASA MOD16A3GF Collection 6.1 at 500 m resolution. Copernicus GLO-30 provides centre elevation and a local slope estimate based on elevation at ±250 m in the east-west and north-south directions [15]. ESA WorldCover 2020 provides descriptive fractions of tree cover, grassland, cropland, built-up area, water, and other land-cover classes in 100 systematic samples per grid [16]. WorldCover 2020 is observed at the end of the study period and is used for descriptive heterogeneity rather than as a baseline causal control. Table 1 summarizes the data sources, spatial and temporal resolutions, variables, and analytical roles.

Table 1. Data sources and analytical roles

Dataset	Resolution/period	Variables	Role
Core grid panel	1 km; summers 2012–2021	LST, NDVI, boundary-area ratio	Outcome and focal exposure
ERA5	0.25°; daily, aggregated Jun–Aug	Air temperature, precipitation, radiation, wind, humidity	Time-varying weather controls
MOD16A3GF C6.1	500 m; annual 2012–2021	ET, PET, latent heat flux, QC	Supplementary mechanism tests
Copernicus GLO-30	30 m; static DSM	Elevation and local slope	Spatial description; absorbed by grid FE
ESA WorldCover 2020	10 m; 2020	Tree, grass, built-up, water fractions	Descriptive heterogeneity only

Notes: LST = land surface temperature; NDVI = Normalized Difference Vegetation Index; ET = evapotranspiration; PET = potential evapotranspiration; FE = fixed effects; DSM = digital surface model.

DOI: 10.54254/2755-2721/2027.MA38676

3.3. Descriptive statistics

Table 2. Descriptive statistics by city

City	Grids	Obs.	LST, °Cmean (SD)	NDVImean (SD)	Air temp., °C	Precip., mm
Berlin	888	8,880	27.47 (3.25)	0.611 (0.133)	19.35	195.5
Budapest	512	5,120	32.49 (2.46)	0.531 (0.136)	21.98	171.8
Vienna	418	4,156	30.05 (3.17)	0.543 (0.186)	21.18	203.2
All cities	1,818	18,156	29.48 (3.71)	0.573 (0.152)	20.51	190.6

Notes: Air temperature and precipitation are the summer ERA5 aggregates at each grid-year. The all cities row is observation-weighted.

As shown in Table 2, Berlin has the highest mean NDVI (0.611) and the lowest mean summer LST (27.47 °C). Budapest has the highest mean LST (32.49 °C), the highest matched summer air temperature, and the lowest summer precipitation among the three cities. Vienna has the largest cross-sectional dispersion in NDVI. These unconditional differences are the reason why we have city-by-year fixed effects, as we would otherwise attribute broad climatic and urban-form differences to vegetation.

3.4. Baseline fixed-effects model

At this level, the preferred specification is:

$$\mathrm{LST}_{ict} = \beta \mathrm{NDVI}_{ict} + \gamma' \mathrm{W}_{ict} + \alpha_i + \delta_{ct} + \varepsilon_{ict} \quad (1)$$

Here i indexes grids, c cities, and t years. W contains summer air temperature, precipitation, shortwave radiation, wind speed, and relative humidity. Grid fixed effects (α_i) absorb all time-invariant local characteristics, including long-run centrality, elevation, slope, water proximity, and persistent urban form. City-by-year fixed effects (δ_{ct}) absorb citywide annual changes in climate, policy, and data processing. Identification therefore comes from deviations in a grid's NDVI relative to its own long-run level and relative to the citywide pattern in that year.

NDVI is divided by 0.1 before estimation, so β is interpreted as the LST difference associated with a 0.1 increase in NDVI. Standard errors are clustered by grid to allow serial correlation and heteroskedasticity within cells. The area-weighted model uses the administrative boundary fraction as an analytical weight.

3.5. Robustness, mechanism, and heterogeneity

Robustness tests restrict the sample to grids with at least 80% of area inside the city boundary; only grids observed in all ten years are retained; winsorize LST and NDVI at the city-specific 1st and 99th percentiles, replace contemporaneous NDVI with its one-year lag and calculate Driscoll–Kraay standard errors. Mechanism analysis first regresses MODIS ET or latent heat flux on NDVI using the same fixed-effects structure then adds ET to LST equation (at least three valid subsamples from MODIS are required and a MODLAND good-quality fraction of at least 0.5). Heterogeneity is tested with city-specific models and interactions between NDVI and above-median 2020 built-up or tree-cover fractions within each city.

DOI: 10.54254/2755-2721/2027.MA38676

4. Results

4.1. Residualized relationship

Figure 2 shows the within-grid relationship after removing grid means and city-year means. All three panels show a clear negative gradient. The binned relationship is sharpest in Budapest and shallower in Berlin, as expected for the city-specific coefficient estimates.

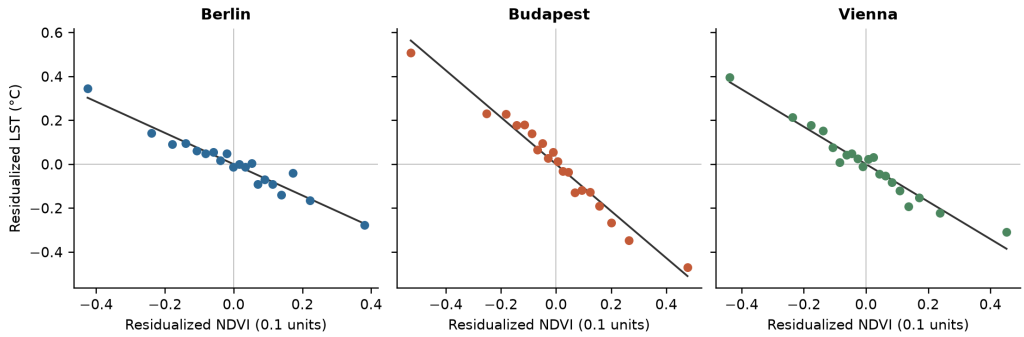


Figure 2. Residualized binned relationship between NDVI and LST

Note: Variables are residualized with respect to grid and city-year means. Points are means of 20 different quantile bins in the city. The lines are fitted with the bin means and are descriptive estimators, not separate estimators.

4.2. Exploratory mechanisms

Table 3. Exploratory mechanisms

	(1)	(2)	(3)	(4)
	Convenience	Park use	Stress recovery	Well-being
Longer walkingdistance	-0.712***	-0.625***	-0.375***	-0.057
	(0.112)	(0.114)	(0.112)	(0.095)
Busy-road barrier	-0.356***	-0.471***	-0.279***	-0.133*
	(0.082)	(0.085)	(0.100)	(0.074)
Perceivedconvenience				0.153
				(0.098)
Park-uselikelihood				0.006
				(0.088)
Expected stressrecovery				0.316***
				(0.078)
Individual fixedeffects	Yes	Yes	Yes	Yes
Respondents	104	104	104	104
Observations	312	312	312	312
Within R-squared	0.210	0.174	0.068	0.286

DOI: 10.54254/2755-2721/2027.MA38676

*Notes: Columns (1) -(3) assess intermediate outcomes and add them to our well-being model. These are purely exploratory and not causal mediation. * p<0.10, ** p<0.05, *** p<0.01.*

As shown in Table 3, longer walking distance is negatively associated with convenience, park use, and expected stress recovery. The busy-road barrier is also negatively associated with all three intermediate outcomes and with well-being.

In the well-being specification, perceived convenience and park-use likelihood are not significant, and expected stress recovery is positively associated with well-being (coefficient = 0.316, SE = 0.078, p<0.01). As our models are exploratory, we cannot interpret our estimates as causal mediators.

4.3. Robustness

Table 4. Robustness checks

Specification	Coef.	SE	p	N	Interpretation
Inside-area ratio ≥ 0.80	-0.835	0.034	0.000	17,147	Contemporaneous estimate stable
Balanced 10-year grids	-0.836	0.033	0.000	18,070	Contemporaneous estimate stable
One-year lagged NDVI	0.046	0.029	0.114	16,338	Not statistically significant
City-specific 1/99 winsorization	-0.835	0.033	0.000	18,156	Contemporaneous estimate stable
Driscoll–Kraay inference	-0.835	0.086	0.000	18,156	Larger SE; conclusion unchanged

Note: Coefficients refer to a 0.1-unit NDVI increase. All models include the preferred controls and fixed effects unless the specification states otherwise.

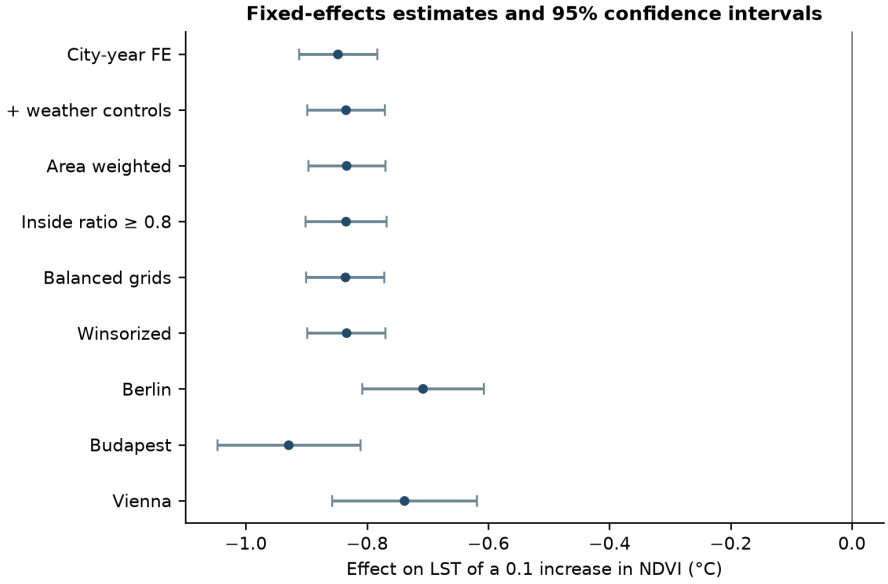


Figure 3. Comparison of fixed-effects estimates

Notes: Points are coefficients for a 0.1 increase in NDVI; bars are 95% confidence intervals (covariance estimator reported) based on the covariance estimator The lagged-NDVI model is excluded because its exposure timing differs.

DOI: 10.54254/2755-2721/2027.MA38676

As shown in Table 4, the interior-grid restriction, balanced-panel sample, winsorization, and alternative inference produce nearly identical point estimates. Driscoll-Kraay standard errors are more than twice the grid-clustered standard errors, but the preferred coefficient remains precisely different from zero. The lagged-NDVI coefficient is 0.046 (SE = 0.029, p = 0.114) but does not therefore corroborate a persistent predictive cooling effect either. This is the most important caution in the robustness analysis: it may be because vegetation dynamics are rapid; measurement and compositing differences across years; or contemporaneous feedback between thermal and vegetation conditions. It also precludes the contemporaneous coefficient from being interpreted as a definitive causal treatment effect. Figure 3 compares fixed-effects estimates across robustness specifications.

4.4. Evapotranspiration mechanism

Table 5. Supplementary evapotranspiration mechanism tests

Model	Dependent variable	NDVI coef.	NDVI SE	ET coef. (SE)	N
NDVI → annual ET	Annual ET (mm)	36.479	2.584	—	2,852
NDVI and ET → LST	LST (°C)	-0.861	0.079	-0.0018 (0.0005)	2,852
NDVI → latent heat	Latent heat (MJ/m^2/day)	0.244	0.017	—	2,852

Note: The mechanism sample must contain at least three valid subsamples of MODIS and MODLAND good quality fraction ≥ 0.5. All displayed NDVI and ET coefficients are statistically significant (p<0.01).

In Table 5 we see that for every 0.1 increase in NDVI there is 36.48 mm more annual ET and 0.244 MJ/m2/day more latent heat flux in the quality-screened sample. ET enters LST model as −0.00178 °C per annual millimetre (SE = 0.00046) evaporative cooling; the coefficient of NDVI does not attenuate relative to preferred baseline (−0.861 °C). So evidence exists for an NDVI–evapotranspiration link and a negative ET–LST association but not clean statistical mediation.

The mechanism sample is also biased. MOD16A3GF has fill values over many impervious urban pixels: only 7,549 panel observations have any valid ET estimate and the strict quality filter leaves 2,852 observations; annual scale is coarser than June–August result. These facts mean Table 5 should be treated as supplementary evidence rather than the paper's main identification result.

4.5. Heterogeneity

Table 6. Heterogeneity in the NDVI–LST association

Subsample/group	Effect	SE / interaction SE	p	N
Berlin	-0.708	0.051	<0.001	8,880
Budapest	-0.930	0.060	<0.001	5,120
Vienna	-0.739	0.061	<0.001	4,156
Low built-up group	-0.954	0.038	<0.001	18,156
High built-up group	-0.491	Interaction SE = 0.050	<0.001†	18,156
Low tree-cover group	-0.861	0.038	<0.001	18,156
High tree-cover group	-0.766	Interaction SE = 0.052	0.071†	18,156

DOI: 10.54254/2755-2721/2027.MA38676

Notes: Effect is the estimated LST difference for a 0.1 increase in NDVI. †p refers to interaction term between high and low groups. Group classifications are city-specific medians of ESA WorldCover 2020 (descriptive because stratifier is measured near end of panel).

As Table 6 shows the association is negative in all three cities and largest in Budapest (point estimate ~31% larger in magnitude than in Berlin). Built-up interaction is positive (0.463 SE = 0.050): cooling slope smaller in high built-up grids (−0.491 °C per 0.1 NDVI vs −0.954 °C in low built-up grids), which fits with less soil volume, moisture availability or vegetation quality in more impervious settings although end of period land cover measure precludes a causal interpretation. Tree-cover interaction is smaller and only marginally significant (p = 0.071).

5. Discussion

5.1. Interpretation and contribution

The preferred estimate shows panel evidence that summers with more vegetation greenness within a 1 km grid are cooler at the land surface (after removing persistent location information and city-specific annual shocks). Its value of about 0.84 °C per 0.1 NDVI is large and should not be mechanically compared to park versus built temperature differences because these are cross-sectional differences between land-cover types and vary by several degrees whereas our coefficient accounts for incremental variation within grid in mixed urban area.

This result complements cross-sectional remote sensing studies in two ways. First the large reduction from -2.54 °C under common year effects to -0.85 °C under city-by-year effects indicates the importance of city specific temporal confounding and second stability across area weighting, boundary restrictions, balanced grids and winsorization suggests that it is not driven by administrative edge cells or very few extreme observations. Cross-city comparison also supports hypothesis that background climate and urban form condition cooling performance.

The mechanism results are consistent with the surface energy pathway: greener observations have higher ET and latent heat flux; ET is not positively correlated with LST. But without coefficient attenuation and because of the selection of ET samples evapotranspiration cannot be considered a mediator (mechanism consistent evidence). There are also channels for shading, albedo and vegetation–building interactions.

5.2. Planning implications

There are three planning implications. First, citywide green-area targets should be complemented by spatial targeting. The within-grid design implies that changes in vegetation condition or abundance can matter even after permanent neighborhood differences are removed. Second, the weaker slope in highly built-up grids warns that adding small areas of low-quality vegetation may not generate the cooling obtained in less impervious areas. Effective interventions may require adequate rooting volume, irrigation or stormwater access, canopy-based design, and connections among green patches. Third, differences in cities make it not feasible to transfer one cooling coefficient across Europe. Local climate, species composition, water supply, and urban geometry should be taken into consideration in the design of the implementation and performance of activities.

We are not looking at surface temperature, but rather pedestrian air temperature or thermal comfort levels. LST is important for radiative and conductive heat loads and can provide spatial information not available from sparse stations, but planning claims about the human exposure under

DOI: 10.54254/2755-2721/2027.MA38676

consideration need to be backed up by air temperature, mean radiant temperature, or population-weighted data.

5.3. Limitations and future research

The study has six main weaknesses. First, contemporaneous NDVI may be endogenous to the same summer weather and compositing conditions that drive LST; city-by-year effects and ERA5 controls reduce this concern but don't eliminate it and insignificant lagged estimate reinforces caution in interpretation. Second, LST and NDVI processing metadata are not included in the supplied core panel. In a final submission satellite platform and product, atmospheric and emissivity correction, cloud and shadow masks, quality thresholds, valid observation counts and annual compositing rule should be documented.

Third, NDVI measures greenness but not green-space type (canopy height, species), irrigation or spatial configuration. Time varying Copernicus imperviousness, Urban Atlas classes, building height, tree cover density, EVI, NDWI, NDBI and landscape metrics would sharpen the analysis; fourth ERA5 is much coarser than 1 km panel; it controls regional meteorology not street scale weather; fifth MOD16 ET is annual and missing over many impervious surfaces; summer MOD16A2GF, Landsat surface moisture or energy-balance ET are preferable; sixth the sample has only three cities so cannot establish representativeness for all European climatic regions.

The strongest next step is a quasi-experimental design. Geocoded Park openings, tree planting programs, green roof mandates or neighborhood greening projects could be used for event study or difference in differences estimates with the same grid framework. Lead coefficients, pre-trend tests and matched untreated grids would separate policy induced greening from ordinary vegetation–temperature co-movement.

6. Conclusion

Based on 18,156 observations from one-kilometre grids in Berlin, Budapest and Vienna from 2012 to 2021, we find that there is a persistent negative contemporaneous association between urban greenness and summer LST. In our preferred model, a 0.1 increase in NDVI is associated with a 0.835 °C decrease in LST. Our result holds for different sample and inference choices and is valid in all three cities. There is also evidence of an evapotranspiration pathway, and the cooling slope is lower in very built-up grids.

These results support urban greening as a locally relevant heat-mitigation strategy, as it is a significant and healthy land cover and not simply some green cover. In addition, the insignificant lagged NDVI model and incomplete remote-sensing data are not sufficient for a causal picture to be established. The paper thus presents a clear basis for the comparison of multi-city panel data and a clear agenda for integrating satellite data with the need for policy-based identification.

7. Data availability

The analytical panel, variable dictionary, descriptive statistics, regression results, and source metadata are included in the research package. ERA5 is produced by Copernicus Climate Change Service; MOD16A3GF is a NASA MODIS product, and Copernicus GLO-30 and ESA WorldCover are publicly available geospatial products. Redistribution and citation should follow the respective provider terms.

DOI: 10.54254/2755-2721/2027.MA38676

References

[1] Oke, T. R. (1982). The energetic basis of the urban heat island. *Quarterly Journal of the Royal Meteorological Society, 108*(455), 1–24. https://doi.org/10.1002/qj.49710845502

[2] Voogt, J. A., & Oke, T. R. (2003). Thermal remote sensing of urban climates. *Remote Sensing of Environment, 86*(3), 370–384. https://doi.org/10.1016/S0034-4257(03)00079-8

[3] Santamouris, M. (2014). On the energy impact of urban heat island and global warming on buildings. *Energy and Buildings, 82*, 100–113. https://doi.org/10.1016/j.enbuild.2014.07.022

[4] Peng, S., Piao, S., Ciais, P., et al. (2012). Surface urban heat island across 419 global big cities. *Environmental Science & Technology, 46*(2), 696–703. https://doi.org/10.1021/es2030438

[5] Clinton, N., & Gong, P. (2013). MODIS detected surface urban heat islands and sinks: Global locations and controls. *Remote Sensing of Environment, 134*, 294–304. https://doi.org/10.1016/j.rse.2013.03.008

[6] Weng, Q., Lu, D., & Schubring, J. (2004). Estimation of land surface temperature–vegetation abundance relationship for urban heat island studies. *Remote Sensing of Environment, 89*(4), 467–483. https://doi.org/10.1016/j.rse.2003.11.005

[7] Estoque, R. C., Murayama, Y., & Myint, S. W. (2017). Effects of landscape composition and pattern on land surface temperature: An urban heat island study in the megacities of Southeast Asia. *Science of the Total Environment, 577*, 349–359. https://doi.org/10.1016/j.scitotenv.2016.10.195

[8] Bowler, D. E., Buyung-Ali, L., Knight, T. M., & Pullin, A. S. (2010). Urban greening to cool towns and cities: A systematic review of the empirical evidence. *Landscape and Urban Planning, 97*(3), 147–155. https://doi.org/10.1016/j.landurbplan.2010.05.006

[9] Gunawardena, K. R., Wells, M. J., & Kershaw, T. (2017). Utilising green and blue space to mitigate urban heat island intensity. *Science of the Total Environment, 584–585*, 1040–1055. https://doi.org/10.1016/j.scitotenv.2017.01.158

[10] Ziter, C. D., Pedersen, E. J., Kucharik, C. J., & Turner, M. G. (2019). Scale-dependent interactions between tree canopy cover and impervious surfaces reduce daytime urban heat during summer. *Proceedings of the National Academy of Sciences, 116*(15), 7575–7580. https://doi.org/10.1073/pnas.1817561116

[11] Schwaab, J., Meier, R., Mussetti, G., et al. (2021). The role of urban trees in reducing land surface temperatures in European cities. *Nature Communications, 12*, 6763. https://doi.org/10.1038/s41467-021-26768-w

[12] Mu, Q., Zhao, M., & Running, S. W. (2011). Improvements to a MODIS global terrestrial evapotranspiration algorithm. *Remote Sensing of Environment, 115*(8), 1781–1800. https://doi.org/10.1016/j.rse.2011.02.019

[13] Norton, B. A., Coutts, A. M., Livesley, S. J., Harris, R. J., Hunter, A. M., & Williams, N. S. G. (2015). Planning for cooler cities: A framework to prioritise green infrastructure to mitigate high temperatures in urban landscapes. *Landscape and Urban Planning, 134*, 127–138. https://doi.org/10.1016/j.landurbplan.2014.10.018

[14] Hersbach, H., Bell, B., Berrisford, P., et al. (2020). The ERA5 global reanalysis. *Quarterly Journal of the Royal Meteorological Society, 146*(730), 1999–2049. https://doi.org/10.1002/qj.3803

[15] European Space Agency & Airbus. (2022). Copernicus DEM [Data set]. https://doi.org/10.5270/ESA-c5d3d65

[16] Zanaga, D., Van De Kerchove, R., De Keersmaecker, W., et al. (2021). ESA WorldCover 10 m 2020 v100. https://doi.org/10.5281/zenodo.5571936